

Resin Selection Criteria for "Tough" Composite Structures

C. C. Chamis* and G. T. Smith†
NASA Lewis Research Center, Cleveland, Ohio

Resin selection criteria are derived using a structured methodology consisting of an upward integrated mechanistic theory and its inverse (top-down structured theory). These criteria are expressed in a "criteria selection space," which can be used to identify resin bulk properties for improved composite "toughness." The resin selection criteria correlate with a variety of experimental data including laminate strength, elevated temperature effects, and impact resistance.

Nomenclature

A	= laminate axial stiffness
C	= global damping matrix; laminate stiffness matrix; stress wave speed
D	= laminate bending stiffness
E	= elastic properties matrix; modulus
ϵ	= failure strain
F	= global force; failure criterion function
\mathcal{F}	= hygrothermal property degradation factor
G	= shear modulus
I	= identity matrix
i	= index
\mathcal{J}	= ply stress influence coefficient
K	= global stiffness matrix; coupling coefficient in failure criterion
k	= volume ratio
M	= global mass matrix; laminate moment
m	= moisture
N	= laminate in-plane force
N_l	= number of layers in a laminate
R	= ply orientation matrix; impacting sphere radius
S	= strength
T	= temperature
t	= thickness
u	= global displacement
x, y, z	= global (structural axes) coordinates
$1, 2, 3$	= ply material axes coordinates
α, β	= thermal and moisture expansion coefficients, respectively
β_{cs}	= strength coefficient-longitudinal compression
γ	= global damping matrix proportionality factor
Δ	= change
δ	= local indentation
ϵ	= strain
ϵ_0	= global reference plane strain
κ	= global curvatures
λ	= eigenvalue; resin selection criteria ratio
ν	= Poisson's ratio
ρ	= density
σ	= stress
φ	= nondimensional function defined by appropriate equations
ω	= circular frequency

Subscripts

C	= compression
c	= composite property
f	= fiber
HTM	= hygrothermomechanical effect
l	= ply property
m	= moisture, hygrothermal effects
r	= resin property
S	= shear
s	= sphere
T	= tension; temperature
v	= void
x, y, z	= respective coordinate directions, properties
0	= reference property
$1, 2, 3$	= ply material axes respective properties
α, β	= T tension or C compression

Matrices

$[]$	= array
$\{ \}$	= vector, column
$[]^{-1}$	= inverse
$[]^T$	= transpose

Introduction

IT is well known in the fiber composite community that resins (matrices) provide the composite with the capability to resist load by keeping the fibers in place. The capability of the resin to keep the fibers in place results from a combination of chemical, thermal, and mechanical interactions. These combined interactions produce the in situ resin physical, hygral, thermal, and mechanical properties that provide the composite with the requisite structural integrity in service environments in general, and in turbine engine service environments in particular. A structural methodology is needed that can be used, in a formal way, to identify bulk (neat) resin characteristics which translate to quantifiable composite structural/mechanical behavior. The result of such structured methodology will be a set of criteria (guidelines) which can be used in advance to screen and/or select resins with the desirable bulk properties in order to provide the specified composite properties. The objective of the present paper is to describe a new structured methodology developed at Lewis for assessing, evaluating, and identifying desirable bulk resin characteristics for specified structural composite integrity (fatigue resistance, fracture toughness, impact resistance, compressive strength, buckling resistance, vibration frequencies, and toughness).

The structured methodology is based on an upward integrated mechanistic theory consisting of composite micromechanics, composite macromechanics, laminate theory, and structural/stress analyses and its inverse (a top-

Received May 1, 1983; presented as Paper 83-0801 at the AIAA/ASME/ASCE/AHS 24th Structures, Structural Dynamics and Materials Conference, Lake Tahoe, Nev., May 2-4, 1983; revision received Sept. 10, 1984. This paper is declared a work of the U.S. Government and therefore is in the public domain.

*Aerospace Structures/Composites Engineer. Associate Fellow AIAA.

†Aerospace Engineer, Retired.

down structured theory). All these are used formally to identify the resin characteristics which have a significant effect on composite mechanical behavior. The structured methodology is developed by using mainly matrix notation. Expanded equations are summarized in figures with appropriate schematics to illustrate the simulation and define the notation. The notation is also summarized for convenience. The structured methodology is based on Lewis research activities on this subject during the past decade (for example, Refs. 1-3). The references cited in the text refer mainly to Lewis research. However, these references include relevant references from the literature. The results obtained are summarized in convenient criteria as simple equation or ratio form which can be used to select resins a priori for improved and/or specific composite toughness.

Structured Methodology

The structured methodology used to develop the resin selection criteria embodies composite micromechanics, composite macromechanics, combined stress failure criteria, laminate theory, and structural/stress analysis. The structured methodology is integrated from composite mechanics upward to structural analysis in order to relate the structural response to constituent materials (fibers and matrix). It is then used in reverse, top-down, from structural response to composite micromechanics. The structured methodology is described herein using a top-down approach in order to relate formally a specific structural response (for example, displacement, stress intensity, stress wave propagation, impact resistance) to constituent material properties (fibers and resins). Resin and matrix are used interchangeably throughout this discussion.

Structural Response

The mathematical model describing the general structural response of a structure is given, using matrix notation, by

$$[M]\{\ddot{u}\} + [C]\{\dot{u}\} + [K]\{u\} = \{F(t)\} \quad (1)$$

where $\{\ddot{u}\}$, $\{\dot{u}\}$, and $\{u\}$ are the acceleration, velocity, and displacement vectors, respectively; $[M]$, $[C]$, and $[K]$ the mass, structural damping, and stiffness matrices, respectively; and $\{F(t)\}$ the time-dependent force vector. The natural frequencies and buckling resistance (buckling load) of a structure are described by special cases of Eq. (1), respectively,

$$\langle [K] - \omega^2 [M] \rangle = [0] \quad (2)$$

$$\langle [K] - \lambda^2 [I] \rangle = [0] \quad (3)$$

where ω is the structure's natural frequency associated with a specific vibration mode, λ the eigenvalue containing the buckling load of a specific buckled shape, and $[I]$ the identity or unit matrix. If it is further assumed that $[C]$ is proportional to $[K]$, ($[C] = \gamma[K]$) prior to any damage, then Eq. (1) can be written

$$[M]\{\ddot{u}\} + \gamma[K]\{\dot{u}\} + [K]\{u\} = \{F(t)\} \quad (4)$$

Equations (2) and (4) depend on composite material properties embodied primarily in $[M]$ and $[K]$, while Eq. (3) depends only on $[K]$. For most structural epoxies the density is about the same.⁴ Therefore, the major influence of the resin in the global structural response of a composite structure is through the stiffness matrix $[K]$.

The global structural stiffness matrix $[K]$ is an assemblage of local stiffnesses. The local stiffnesses are related to the force deformation relationships and the local geometry. The force deformation relationships for a composite laminate, in-

cluding hygral (moisture) and thermal forces, are given by²

$$\begin{Bmatrix} \{N\} \\ \{M\} \end{Bmatrix} = \begin{bmatrix} [A] & [C] \\ [C]^T & [D] \end{bmatrix} \begin{Bmatrix} \{\epsilon_0\} \\ \{\kappa\} \end{Bmatrix} - \begin{Bmatrix} \{N_T\} \\ \{M_T\} \end{Bmatrix} - \begin{Bmatrix} \{N_M\} \\ \{M_M\} \end{Bmatrix} \quad (5)$$

where $\{N\}$ and $\{M\}$ are the resultant force and moment vectors at the section, respectively. The subscripts T and M denote thermal and moisture forces. The reference-plane strain vector is given by $\{\epsilon_0\}$ and the local curvatures by $\{\kappa\}$. The arrays $[A]$, $[C]$, and $[D]$ denote axial, coupled, and bending stiffnesses, respectively. The various arrays on the right side of Eq. (5) for an N_i ply laminate, using laminate theory,⁵ are given by

$$\begin{aligned} [A], [C], [D] &= \sum_{i=1}^{N_i} \langle [(Z_i - Z_b), 1/2(Z_i^2 - Z_b^2), 1/3(Z_i^3 - Z_b^3)] \\ &\quad \times [R]^T [E]^{-1} [R] \rangle_i \\ \{N_T\}, \{M_T\} &= \sum_{i=1}^{N_i} \langle [(Z_i - Z_b), 1/2(Z_i^2 - Z_b^2)] \\ &\quad \times \Delta T [R]^T [E] \{\alpha\} \rangle_i \\ \{N_M\}, \{M_M\} &= \sum_{i=1}^{N_i} \langle [(Z_i - Z_b), 1/2(Z_i^2 - Z_b^2)] \\ &\quad \times \Delta m [R]^T [E] \{\beta\} \rangle_i \end{aligned} \quad (6)$$

In Eq. (6), Z locates the i th ply through the thickness from a reference plane, $[R]$ is the strain transformation matrix which defines the i th ply orientation (ply material axes) relative to the structural axes, $[E]$ defines the ply stress-strain relationships, $\{\alpha\}$ the ply thermal expansion coefficients, and $\{\beta\}$ the ply moisture expansion coefficients. The relative changes ΔT and Δm denote the changes in temperature and moisture, respectively, of the i th ply measured from a reference condition. The temperature and the moisture for the i th ply are determined by heat transfer and moisture diffusion analyses.

The important point to note from Eq. (5) is that the resin properties influencing structural response are reflected through the ply property arrays $[E]$, $\{\alpha\}$, and $\{\beta\}$. Another

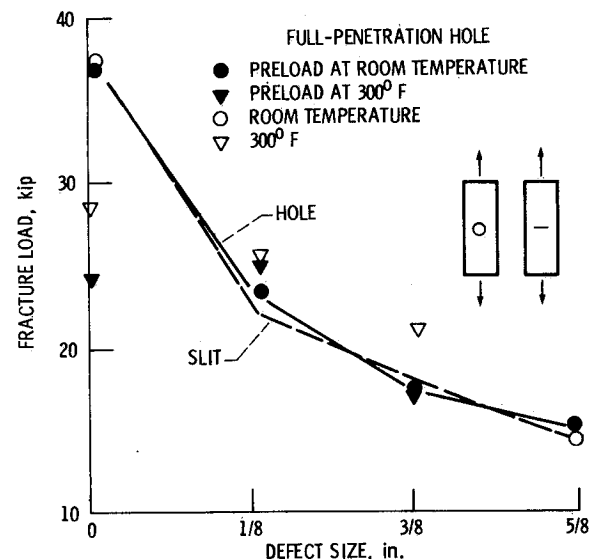


Fig. 1 Static fracture data of composites with defects.

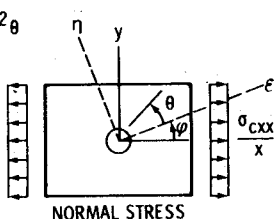
important point to note is that the top-down structured theory described by Eqs. (1-6) predicts global structural response in very good agreement with experimental data. For example: 1) the natural frequencies and mode shapes predicted by Eq. (2) are in excellent agreement with experimental data for fiber composite fan blades⁶ and hybrid composite blades⁷; 2) the buckling loads of anisotropic plates, including bending, stretching, and coupling, predicted by Eq. (3) are in good agreement with experimental data^{8,9}; 3) the impact displacements predicted using Eq. (4) are in good agreement with the high-speed movie data for a large hybrid composite fan blade⁷; and 4) the hygrothermomechanical response of a variety of angle-ply laminates predicted by Eq. (5) are in very good agreement with measured data.² This good agreement of the predicted various structural responses with experimental data verifies that the global structural response of composite structures is formally related to the ply properties $[E]$, $\{\alpha\}$, and $\{\beta\}$ in Eq. (6). These ply properties can be formally related to matrix properties by continuing the top-down structured theory through composite macromechanics, combined-stress failure criteria, and composite micromechanics as will be described later.

Stress Intensity/Concentration

Experimental data from composite laminates with circular holes and slit type defects exhibit the same fracture characteristics. These characteristics are similar for tensile or compressive loads and for a variety of hygrothermal environments.¹⁰ Typical results are shown in Fig. 1. Explicit equations are available which describe the stress concentration/intensity in the vicinity of a circular hole in an infinite composite angle-ply laminate.¹¹ The equations relevant to this top-down structured theory are summarized in Fig. 2 with accompanying schematics.

It can be seen in Fig. 2 that the stress concentration ratio ($\sigma_{c\theta\theta}/\sigma_{c\theta\theta}$) in the vicinity of the hole depends on the laminate properties $E_{c\theta\theta}$, $E_{c\theta\theta}$, $E_{c\theta\theta}$, $G_{c\theta\theta}$, and $\nu_{c\theta\theta}$. These properties are determined using the following laminate theory equation⁵

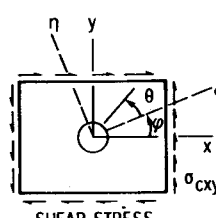
$$[E_c] = \frac{I}{t_c} \sum_{i=1}^{N_f} \langle t[R]^T [E] [R] \rangle_i \quad (7)$$

$$\frac{\sigma_{c\theta\theta}}{\sigma_{c\theta\theta}} = \frac{E_{c\theta\theta}}{E_{c\theta\theta}} \left\{ R_0 [(R_0 + R_{D1}) \sin^2 \varphi] \cos^2 \theta + [1 + (R_0 + R_{D1}) \cos^2 \varphi] \sin^2 \theta - \frac{R_{D1}}{4} (1 + R_0 + R_{D1}) \sin 2\varphi \sin 2\theta \right\}$$


NORMAL STRESS

$$R_0 = \sqrt{E_{c\theta\theta}/E_{c\theta\theta}}$$

$$R_{D1} = \left[2 \left(\frac{E_{c\theta\theta}}{E_{c\theta\theta}} - \nu_{c\theta\theta} \right) + \frac{E_{c\theta\theta}}{G_{c\theta\theta}} \right]^{1/2}$$

$$\frac{\sigma_{c\theta\theta}}{\sigma_{c\theta\theta}} = \frac{E_{c\theta\theta}}{2E_{c\theta\theta}} (1 + R_0 + R_{D1}) \left\{ -R_{D1} \cos 2\varphi \sin 2\theta + [1 + (R_0 + R_{D1}) \cos 2\theta + R_0 - 1] \sin 2\varphi \right\}$$


SHEAR STRESS

NOTE: $\sigma_{c\theta\theta}$ AND $E_{c\theta\theta}$ ARE IN THE HOOP DIRECTION AT θ

Fig. 2 Stress concentrations depend significantly on composite moduli.

where t_c is the laminate thickness and t_i is the ply thickness. Comparing Eqs. (7) and (6), it can be seen by inspection that $[E_c] = [A]/t_c$. Therefore, the stress concentrations in the laminate (composite-structure) are formally related to ply properties through Eq. (7) and the equations in Fig. 2. The hygrothermal effects on the stress concentration are determined from Eq. (5) since the local laminate stresses are related to $\{N\}$ and $\{M\}$, or $\{\epsilon_\theta\}$ and $\{\kappa\}$ as will be described later.

Stress Wave Propagation

The speed (C) of the in-plane stress wave propagation in an angle-ply composite laminate in the X , Y , and XY (shear) directions, respectively, are given by

$$C_x = \left[\frac{gE_{c\theta\theta}}{\rho(I - \nu_{c\theta\theta}\nu_{c\theta\theta})} \right]^{1/2} \quad (8)$$

$$C_y = \left[\frac{gE_{c\theta\theta}}{\rho(I - \nu_{c\theta\theta}\nu_{c\theta\theta})} \right]^{1/2} \quad (9)$$

$$C_{xy} = [(gG_{c\theta\theta}/\rho)]^{1/2} \quad (10)$$

where g is the gravity acceleration, ρ is the laminate density, G is the shear modulus, and the subscripts denote respective directions. The corresponding through-the-thickness normal and shear speeds, respectively, are given by

$$C_z = (gE_{czz}/\rho)^{1/2} \quad (11)$$

$$C_{xz} = (gG_{c\theta\theta}/\rho)^{1/2} \quad (12)$$

$$C_{yz} = (gG_{c\theta\theta}/\rho)^{1/2} \quad (13)$$

The speeds predicted by Eqs. (8-10), (12), and (13) have been correlated with experimental data.¹² These equations have also been used extensively to theoretically investigate stress wave propagation in angle-ply laminates due to normal, oblique, and edge impacts.¹³

Theoretical predictions of stress wave propagation due to point impact require a contact law in general. One such law for an impacting elastic sphere is given by the following approximate relationships.¹⁴

$$F = (4/3)(R_s)^{1/2} \left[\frac{E_s E_{czz}}{E_s + (1 - \nu_s) E_{czz}} \right] \delta^{3/2} \quad (14)$$

$$\mathcal{F}_m = \left[\frac{T_{gr} - T_T}{T_{gr} - T_{ro}} \right]^{1/2}$$

$$E_{\theta 11} = k_f E_{f11} + k_r \mathcal{F}_m E_{ro}$$

$$U_{\theta 12} = U_{\theta 13} = k_f U_{f12} + k_r U_{ro}$$

$$E_{\theta 33} = E_{\theta 22} = \frac{\mathcal{F}_m E_{ro}}{1 - \sqrt{k_f} \left(\frac{1 - \mathcal{F}_m E_{ro}}{E_{f22}} \right)}$$

$$G_{\theta 13} = G_{\theta 12} = \frac{\mathcal{F}_m G_{ro}}{1 - \sqrt{k_f} (1 - \mathcal{F}_m G_{ro}/G_{f23})}$$

$$G_{\theta 23} = G_{\theta 32} = \frac{\mathcal{F}_m G_{ro}}{1 - \sqrt{k_f} (1 - \mathcal{F}_m G_{ro}/G_{f23})}$$

$$U_{\theta 23} = (E_{\theta 22}/2G_{\theta 23}) - 1$$

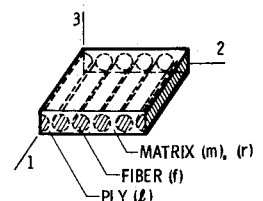


Fig. 3 Governing equations: micromechanics-elastic constants.

$$S_{L11T} = S_{f1} [k_f + k_r E_r / E_{f11}]$$

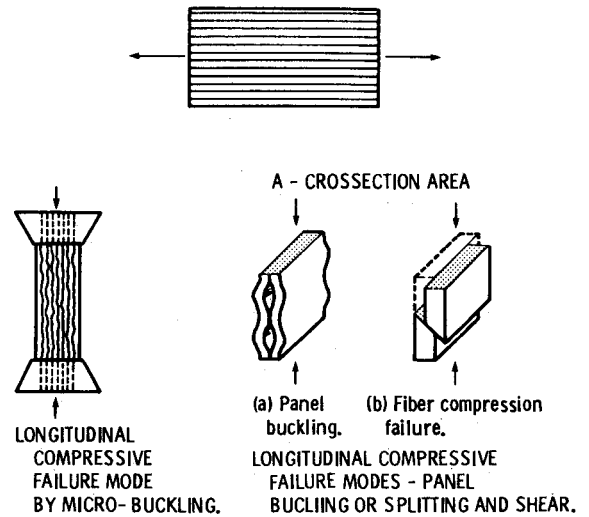
$$S_{L11C} = \min \left\{ \left[\frac{F(k_v) G_r}{(1 - k_f) + k_f G_r / G_{f12}} \right] \right.$$

$$(\beta_{cs} S_{L12S} + S_{rc}),$$

$$\left. S_{fc} k_f + k_r E_r / E_{f11} \right\}$$

$$F(k_v) = \frac{1 - 2 \left(\frac{k_v}{1 - k_f} \right) + \left(\frac{k_v}{1 - k_f} \right)^2}{1 - \left(\frac{k_v}{1 - k_f} \right)}$$

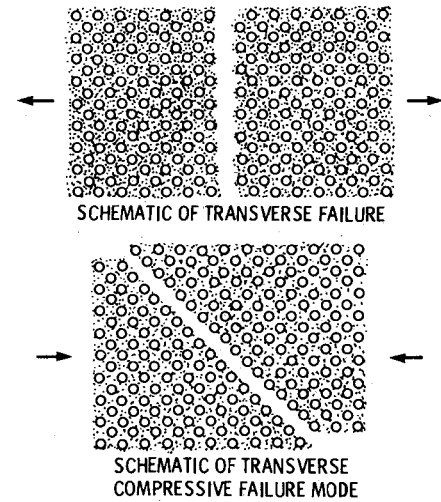
Fig. 4 Governing equation: micro-mechanics-uniaxial tensile and compressive strengths.



TRANSVERSE

$$S_{L22T, C} = \frac{1}{\left[1 - \sqrt{k_f} \left(\frac{1 - E_m}{E_{f22}} \right) \right] \left[1 + \varphi_\eta (\varphi_\eta - 1) + 1/3 (\varphi_\eta - 1)^2 \right]^{1/2}} S_{MT, C}$$

$$\varphi_\eta = \frac{1}{\left(\frac{\pi}{4k_f} \right)^{1/2} - 1} \left[\left(\frac{\pi}{4k_f} \right)^{1/2} - \frac{1}{1 - \sqrt{k_f} \left(\frac{1 - E_m}{E_{f22}} \right)} \left(\frac{E_m}{E_{f22}} \right) \right]$$

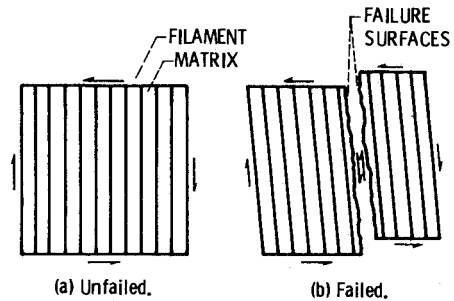


LOWER BOUND

$$S_{L22T, C} = \left[1 - \left(\frac{4k_f}{\pi} \right)^{1/2} \right] S_{MT, C}$$

INTRALAMINAR SHEAR: REPLACE E & S_{MT} WITH G & S_{MS} , RESPECTIVELY

$$\text{VOID EFFECTS: } S_{MV} = \left\{ 1 - [4k_v / (1 - k_f) \pi]^{1/2} \right\} S_M$$



SCHEMATIC OF SHEAR FAILURE MODES (INPLANE, INTRALAMINAR)

Fig. 5 Governing equations: micromechanics-uniaxial transverse and shear strengths.

where F is the contact force, R_s the radius of the impacting sphere, and δ the local indentation. The subscript s denotes impacting sphere properties.

Taken collectively, Eqs. (8-14) show that stress wave propagation in composite laminates depends on the laminate properties E , G , ν , and ρ . These laminate properties are formally related to ply properties through Eq. (6) as was already mentioned.

Ply Strains and Stresses

In the top-down structured theory, the i th ply strains $\{\epsilon_i\}$ are formally related to global variables $\{\epsilon_0\}$ and $\{\kappa\}$ by the

following matrix equation:

$$\{\epsilon_i\} = [R_i] \{ \{\epsilon_0\} - Z_i \{\kappa\} \} \quad (15)$$

where the global variables are determined from structural analysis. The corresponding ply stresses are given by

$$\{\sigma_i\} = [E_i] \{ \{\epsilon_i\} - \Delta m \{\beta\} - \Delta T \{\alpha\} \} \quad (16)$$

For the special case of in-plane loads only, the ply stresses are formally related to laminate stresses $\{\sigma_c\}$ by

$$\{\sigma_i\} = [E_i] [R_i] [E_c]^{-1} \{\sigma_c\} \quad (17)$$

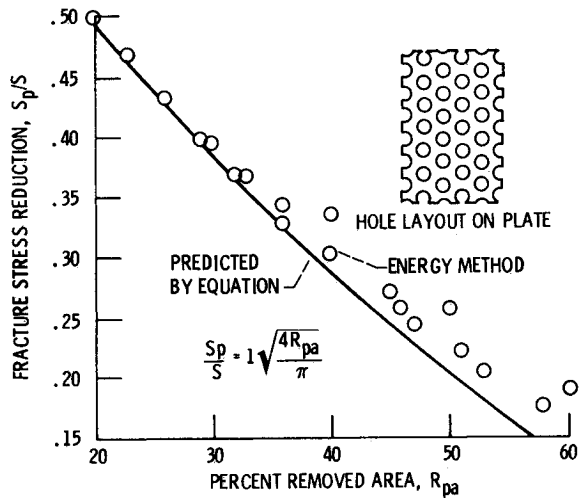


Fig. 6 Simple expression accurately predicts fracture stress reduction in perforated plates compared to energy method.

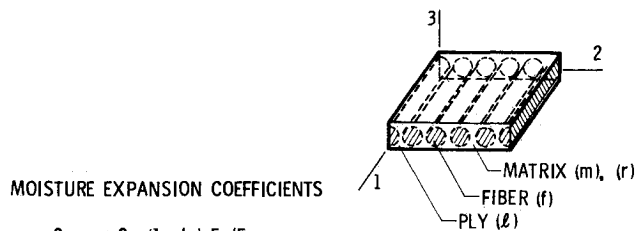


Fig. 7 Governing equations: micromechanics-hygrothermal properties.

$$\mathcal{G}_{L/X} = \frac{E_{L11}}{E_{CXX} (1 - \nu_{L12} \nu_{L21})} [(1 - \nu_{L21} \nu_{CXY}) \cos^2 \theta + (\nu_{L21} - \nu_{CXY}) \sin^2 \theta]$$

$$\mathcal{G}_{T/X} = \frac{E_{L22}}{E_{CXX} (1 - \nu_{L12} \nu_{L21})} [(\nu_{L12} - \nu_{CXY}) \cos^2 \theta + (1 - \nu_{CXY} \nu_{L21}) \sin^2 \theta]$$

$$\mathcal{G}_{S/X} = \frac{G_{L12}}{E_{CXX} (1 - \nu_{L12} \nu_{L21})} [(1 + \nu_{CXY}) \sin^2 \theta]$$

WHERE

$$\sigma_{L11} = \mathcal{G}_{L/X} \sigma_{CXX}; \sigma_{L22} = \mathcal{G}_{T/X} \sigma_{CXX}; \sigma_{L12} = \mathcal{G}_{S/X} \sigma_{CXX}$$

$$\text{AND AT FAILURE } \sigma_{CXX} = S_{CXX}$$

where $[E_c]$ is given by Eq. (7). Equation (17) is significant because it shows that the ply stresses depend on local ply properties $[E_i]$ as well as integrated laminate properties $[E_c]$. Equation (17) constitutes the ply stress influence coefficients for the case of in-plane loads only.

The ply strains and stresses determined from Eqs. (15) and (16), or (17), are normally compared to ply fracture properties using available failure criteria such as ply:

$$\text{maximum strain: } \{\epsilon_i\} \leq \{\xi_i\} \quad (18)$$

$$\text{maximum stress: } \{\sigma_i\} \leq \{S_i\} \quad (19)$$

or combined-failure stress criterion, for example,¹⁵

$$F(\sigma_i, S_i, K_i) = 1 - \left[\left(\frac{\sigma_{i1\alpha}}{S_{i1\alpha}} \right)^2 + \left(\frac{\sigma_{i2\beta}}{S_{i2\beta}} \right)^2 + \left(\frac{\sigma_{i2S}}{S_{i2S}} \right)^2 - K_{i12} \frac{\sigma_{i1\alpha} \sigma_{i2\beta}}{S_{i1\alpha} S_{i2\beta}} \right] \quad (20)$$

where σ_i denotes the i th ply stress along the material axes denoted by the numerical subscripts and with sense denoted by α or β (tension or compression). The corresponding ply uniaxial strengths (fracture stresses) are denoted by S . The coupling coefficient K_{i12} depends on the ply elastic properties E_{i11} , E_{i22} , ν_{i12} , and ν_{i23} .

The ply elastic constants $[E_i]$ and the uniaxial strengths (S_i) can be formally related to matrix material properties using composite micromechanics as will be described subsequently.

Equations (18), (19), and/or (20) are used to assess laminate/composite structural integrity, durability, and/or composite toughness. This may be stated as the magnitude of stress $\{\sigma_c\}$, resulting from stress concentration due to impact or defects, that a composite can sustain prior to ply or interply damage which will degrade either the composite global structural response or the composite life/durability.³ The composite life, or durability, is usually measured by its resistance to impact, cyclic (fatigue), mechanical, hygral, and/or thermal loading.

Composite Micromechanics

Composite micromechanics is the discipline that formally relates ply properties to constituent material properties.⁴

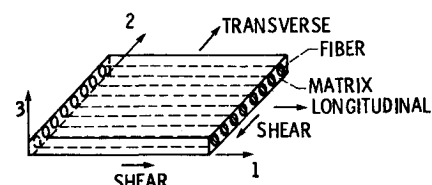
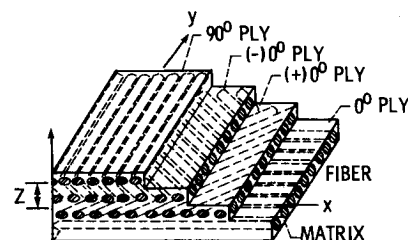


Fig. 8 Ply stress influence coefficients.

$$F(\sigma_\ell, S_\ell, E_\ell, \mathcal{F}_{HTM}) = 1 - \frac{\sigma_{cxx}^2 E_{11}^2}{E_{cxx}^2} \left\{ \frac{1}{S_{11a}^2} \left[(1 - \nu_{\ell 21} \nu_{cxy}) \cos^2 \theta + (\nu_{\ell 21} - \nu_{cxy}) \sin^2 \theta \right]_\alpha^2 \right. \\ + \frac{\mathcal{F}_m^2 E_{22}^2}{\mathcal{F}_{HTM}^2 E_{11}^2 S_{22\beta}^2} \left[(\nu_{\ell 12} - \nu_{cxy}) \cos^2 \theta + (1 - \nu_{cxy} \nu_{\ell 21}) \sin^2 \theta \right]_\beta^2 \\ + \frac{\mathcal{F}_m^2 G_{12}^2}{\mathcal{F}_{HTM}^2 E_{11}^2 S_{12s}^2} \left[(1 + \nu_{cxy}) \sin^2 \theta \right]_s^2 \\ \left. - \frac{\kappa_{12} \mathcal{F}_m E_{22}}{E_{11} S_{11a} \mathcal{F}_{HTM} S_{22\beta}} \left[(1 - \nu_{\ell 12} \nu_{cxy}) \cos^2 \theta + (\nu_{\ell 21} - \nu_{cxy}) \sin^2 \theta \right]_\alpha \right. \\ \left. \times \left[(\nu_{\ell 12} - \nu_{cxy}) \cos^2 \theta + (1 - \nu_{cxy} \nu_{\ell 21}) \sin^2 \theta \right]_\beta \right\} \\ \mathcal{F}_m = \left[\frac{T_{gw} - T}{T_{go} - T_o} \right]^{1/2}; \quad \mathcal{F}_{HTM} = \mathcal{F}_m - B \log_{10} N$$

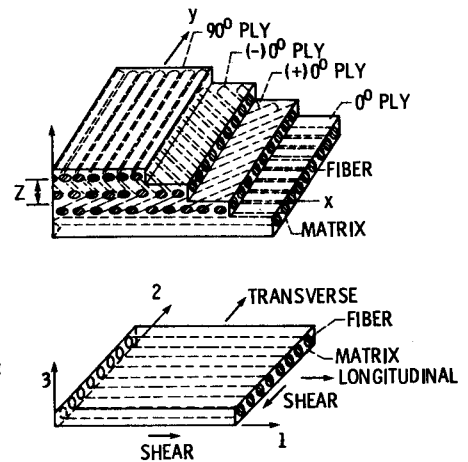


Fig. 9 Ply combined stress failure criterion with hygrothermomechanical effects.

$$\text{TRANSVERSE STRENGTH} \quad S_{\ell 22} = (1 - \sqrt{k_f}) \mathcal{F}_{HTM} S_m \approx C_s S_m$$

$$\text{IF } S_m = \lambda_s S_{mo} \quad (\lambda_s > 1)$$

$$S_{\ell 22} \approx C_s \lambda_s S_{mo}$$

$$\text{TRANSVERSE MODULUS} \quad E_{\ell 22} = \frac{\mathcal{F}_m E_m}{1 - \sqrt{k_f} \left(1 - \frac{\mathcal{F}_m E_m}{E_{f22}} \right)} \approx C_m E_m$$

$$E_m = \lambda_m E_{mo} \quad (\lambda_m > 1)$$

$$E_{\ell 22} = C_m \lambda_m E_{mo}$$

$$\text{ENERGY DENSITY} \quad U_{\ell 22} = \frac{S_{\ell 22}^2}{2E_{\ell 22}} = \frac{C_s^2 \lambda_s^2 S_{mo}^2}{2C_m \lambda_m E_{mo}}$$

$$\text{FIRST PLY FAILURE} \quad S_{cxx} = \left\{ \frac{C_o \mathcal{F}_m (1 - k_f) \left[1 - \sqrt{k_f} \left(1 - \frac{\mathcal{F}_m E_m}{E_{f22}} \right) \right]}{\mathcal{F}_m} \right\} \frac{S_m}{E_m} \\ S_{cxx} \approx C \frac{\lambda_s S_{mo}}{\lambda_m E_{mo}}$$

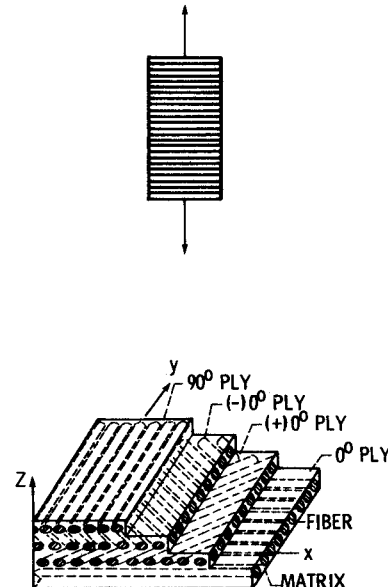


Fig. 10 Benefit bounds equations for resin properties.

The properties pertinent to the development of resin selection criteria pursued herein are the ply mechanical properties (elastic [E_ℓ] and strength S_ℓ) and the ply hygrothermal properties (β_ℓ and α_ℓ) where the subscript ℓ (instead of i) has been used to denote ply properties, in general. In addition, the hygrothermal degradation effects on the mechanical and thermal properties are related to the "hot-wet" ply environment and to the "hot-wet" glass transition temperature of the resin through a hygrothermal degradation factor \mathcal{F}_m (HTM).

The equations for predicting ply properties in terms of constituents are summarized in Fig. 3. The notation in these

equations corresponds to the schematic in the figure. The ply elastic properties are explicitly related to the matrix resin (r) and fiber (f) properties and to the hygrothermal degradation through (\mathcal{F}_m). It can be readily observed in these equations that the resin-controlled ply properties are: $E_{\ell 22}$, $E_{\ell 33}$, $G_{\ell 12}$, and $G_{\ell 23}$. The equations for ply longitudinal strengths (tension and compression) with attendant schematics for various fracture modes are summarized in Fig. 4. The dependence of the ply longitudinal compression strength on resin is through the resin properties (denoted by subscript r) and the ply intralaminar shear strength ($S_{\ell 12s}$). The hygrothermal degradation effects on ply longitudinal

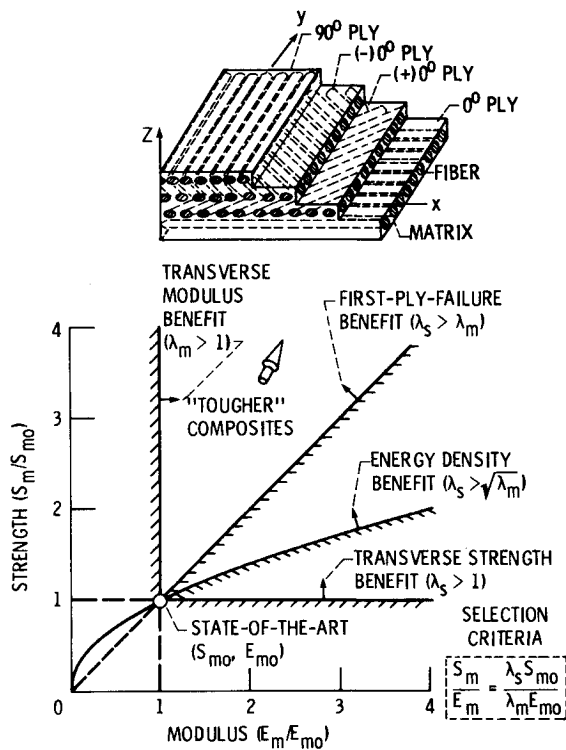


Fig. 11 Resin selection criteria for tougher composites.

strengths are incorporated through the respective resin properties using the degradation factor (\mathcal{F}_m) as shown in Fig. 3. Similarly, the equations for ply transverse (tension and compression) and intralaminar shear properties are summarized in Fig. 5. The equation for lower bound strength is derived assuming a resin slab (plate) perforated with a regular array of holes. The correlation between this equation and experimental data on yield stress of a steel plate¹⁶ is illustrated in Fig. 6, where S_p and S denote yield stresses of the plate with and without the perforations, respectively. The parameter R_{pa} denotes perforated area ratio, which equals K_f or the fiber volume ratio. The corresponding equations for ply hygral (β_l) and thermal (α_l) properties are summarized in Fig. 7.

The equations summarized in Figs. 4-6 close the loop in the structured methodology required to develop the resin selection criteria. Recall that this methodology consists of two multilevel theories: 1) an upward integrated theory formally integrating resin elastic, hygral, and thermal properties into composite structural response and 2) a top-down structured theory formally relating the composite structural integrity/durability to the same resin and, in addition, strength properties. The hygrothermal environment and degradation effects are included in both theories.

Resin Selection Criteria—Derivations and Identifications

The resin selection criteria are derived with the aid of Eqs. (17) and (20). Equation (17) is used in the form of ply stress influence coefficients (PSIC) defined as

$$[\mathcal{J}_l] = [E_l][R_l][E_c]^{-1} \quad (21)$$

where the subscript l is again used to denote ply properties in general. The expanded form of Eq. (2) when the composite is subjected only to σ_{cex} is shown in Fig. 8. Analogous equations can be derived when the composite is subjected to other stresses or combinations.¹⁷ Using the PSIC from the equations in Fig. 8 and Eq. (20) accounting for hygrothermal degradation effects (\mathcal{F}_m) and hygrothermomechanical

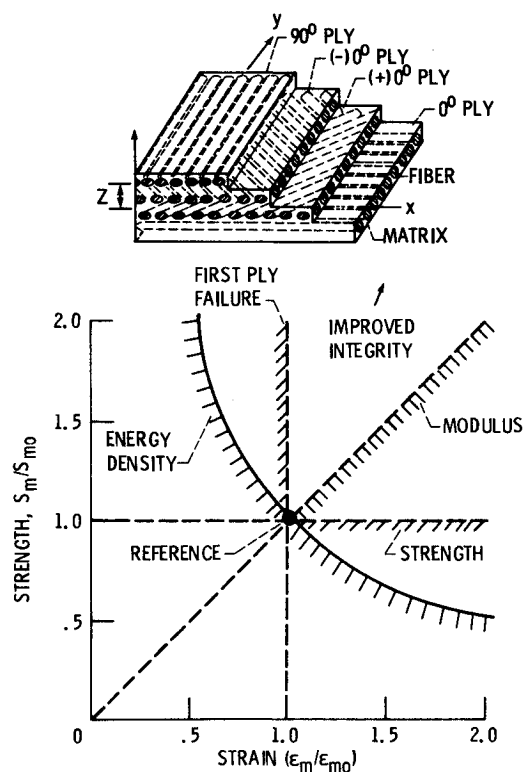


Fig. 12 Resin property regions for improved composite structural integrity.

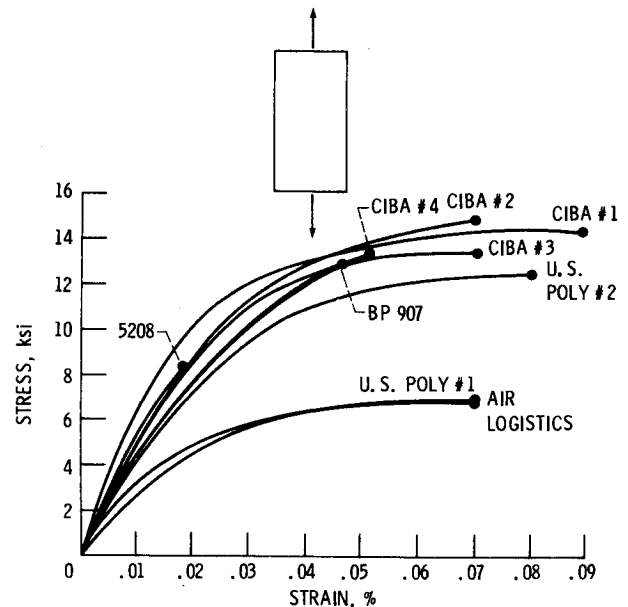


Fig. 13 Average results of tough resin stress-strain curves.

degradation effects (\mathcal{F}_{HTM}), and rearranging results in the equation summarized in Fig. 9. The definitions for \mathcal{F}_m and \mathcal{F}_{HTM} are included at the bottom of the figure for completeness. The equation in this figure explicitly relates ply combined stress failure/damage (first ply failure) to the composite stress and includes the hygrothermomechanical degradation effects. The resin influence is through the properties with subscripts 22 and 12 and can now be readily assessed by expressing these properties in terms of constituent properties using the appropriate composite micro-mechanics equations from Figs. 3-5.

The results obtained for transverse strength, transverse modulus, energy density, and first ply failure, respectively,

are summarized in Fig. 10. All of these are expressed explicitly in terms of matrix properties. The benefits of a matrix (resin) (S_m , E_m) relative to a reference matrix (S_{m0} , E_{m0}) are indicated by λ_s (S_m/S_{m0}) for strength and λ_m (E_m/E_{m0}) for modulus. The meaning of the parameters C_s , C_m , C_0 , and C is apparent from the equations in which they appear. These parameters are used to include those constituent material and ply properties which are independent, or very nearly so, of resin properties. Analogous expressions can be obtained for shear and interply delamination from the expressions in Fig. 10 by suitable replacement of variables and subscripts.

From the previous discussion and the expressions in Fig. 10, the resin selection criteria for improvements in individual properties are:

- 1) λ_s for ply transverse and intralaminar shear strengths, interply delamination, and interlaminar shear controlled longitudinal compression.
- 2) λ_m for ply transverse modulus, longitudinal tensile and shear strengths, and crippling-controlled longitudinal compression strength.
- 3) λ_s/λ_m for ply transverse and intralaminar and interlaminar shear energy densities.
- 4) λ_s/λ_m for laminate (composite) strength and composite toughness in general.

The resin selection criteria are represented graphically in Fig. 11, where the improvements relative to a reference

(state-of-the-art, S_{m0} and E_{m0}) matrix for individual and combined properties are readily observed. The resin selection criteria for improved composite toughness and structural integrity/durability in general can now be simply stated as follows: To improve composite toughness, increase the S_m/E_m ratio relative to S_{m0}/E_{m0} with S_m increasing at a faster rate than E_m .

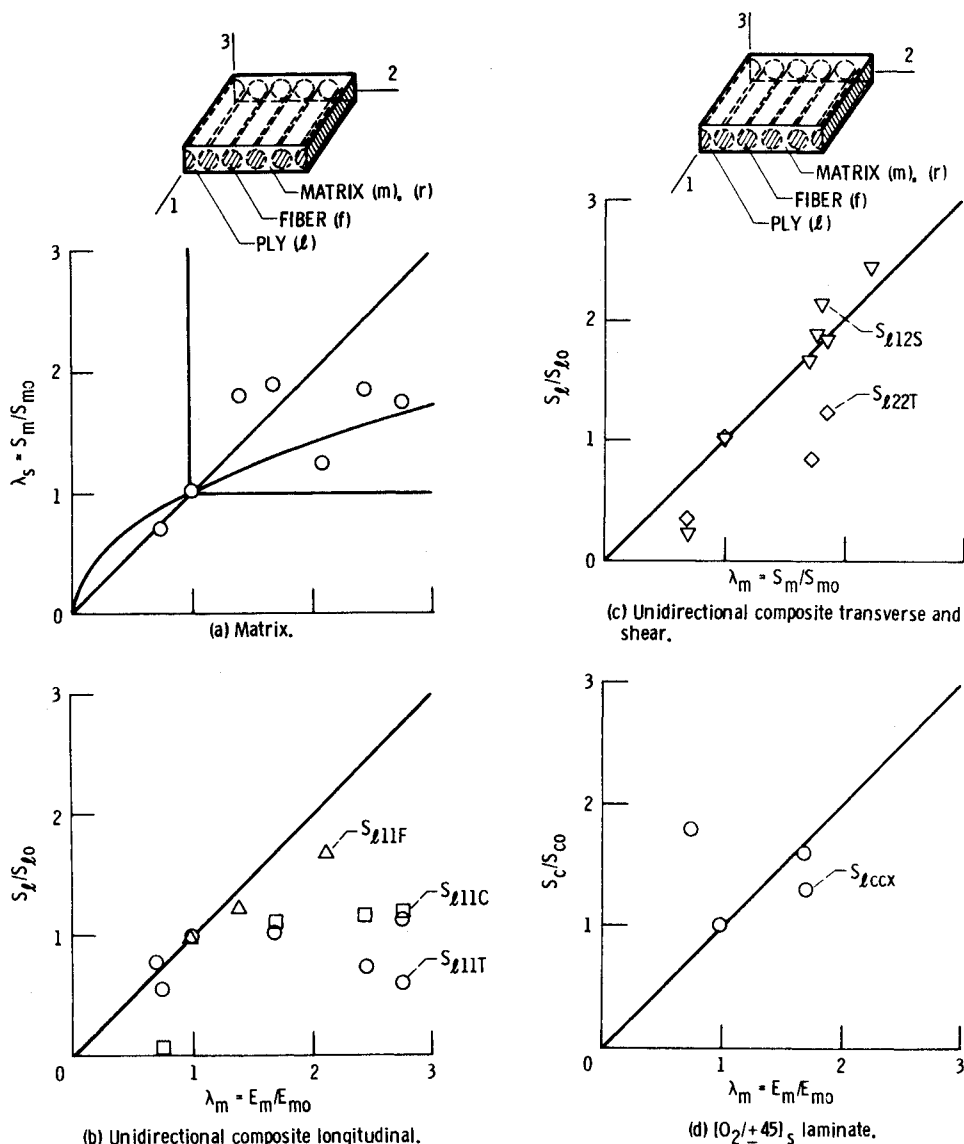
It is important to note that S_m/E_m may be misconstrued as only strain to fracture. *It is not*, as is readily observed from Fig. 12. It is also worth noting that the structural integrity dependence on the (S_m/E_m) ratio is consistent with those obtained by sensitivity analyses in conjunction with structural optimization.¹⁸

Comparison with Experimental Data and Discussion

Available experimental data^{19,20} for several composite properties made from a variety of resins, with stress-strain curves as plotted in Fig. 13 and in different environments, are compared with the resin selection criteria described previously.

Angle-ply laminate and unidirectional strengths and moduli are compared with λ_m and λ_s in Fig. 14. The correlation for resin-controlled properties (transverse and shear) with λ_s is excellent. Also the fiber-controlled strengths S_{LIF} (longitudinal flexure), S_{LIC} , and S_{CCX} correlate with λ_m . As expected, the fiber-controlled property S_{LIT} does not cor-

Fig. 14 Resin selection criteria correlation with measured composite data.



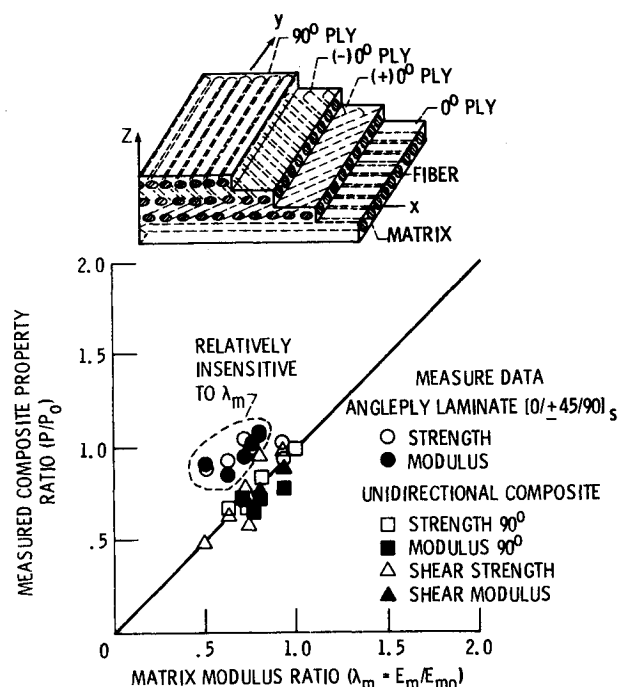


Fig. 15 Proposed resin selection criteria correlate with measured data. P_0 and E_{m0} are reference properties.

relate with λ_m . A very good correlation of resin-controlled properties—90 deg (transverse) and shear—with λ_m only is shown in Fig. 15. Comparisons with elevated temperature data are shown in Fig. 16. Again the correlation of resin-controlled properties (transverse and shear) with λ_s is excellent, while there is no correlation of fiber-controlled properties with λ_m .

Various resins, including those from Fig. 13, are plotted in the resin selection criteria space shown in Fig. 17. It can be seen in this figure that 5208 matrix is below the first ply failure boundary and would, therefore, be unsuitable for improved fracture toughness. However, a group of resins are identified that will improve the composite toughness significantly. These resins have λ_s ratios of about 3 and λ_m of about 2 or λ_s/λ_m of about 1.5. The delaminated area sustained by a composite under impact loading is correlated with the resin selection criteria λ_s/λ_m in Fig. 18. As can be seen, the correlation is excellent.

The important conclusions from the correlation results and discussion is that the "resin selection criteria" derived herein correlate with experimental data for a variety of conditions. The resin selection criteria space is a concise graphic means to a priori identify resins with desirable bulk state characteristics which will lead to tougher composites. The correlation of the criteria with fatigue data is yet to be determined. However, based on the theoretical results, it is anticipated that these resin selection criteria should apply to fatigue loadings as well.

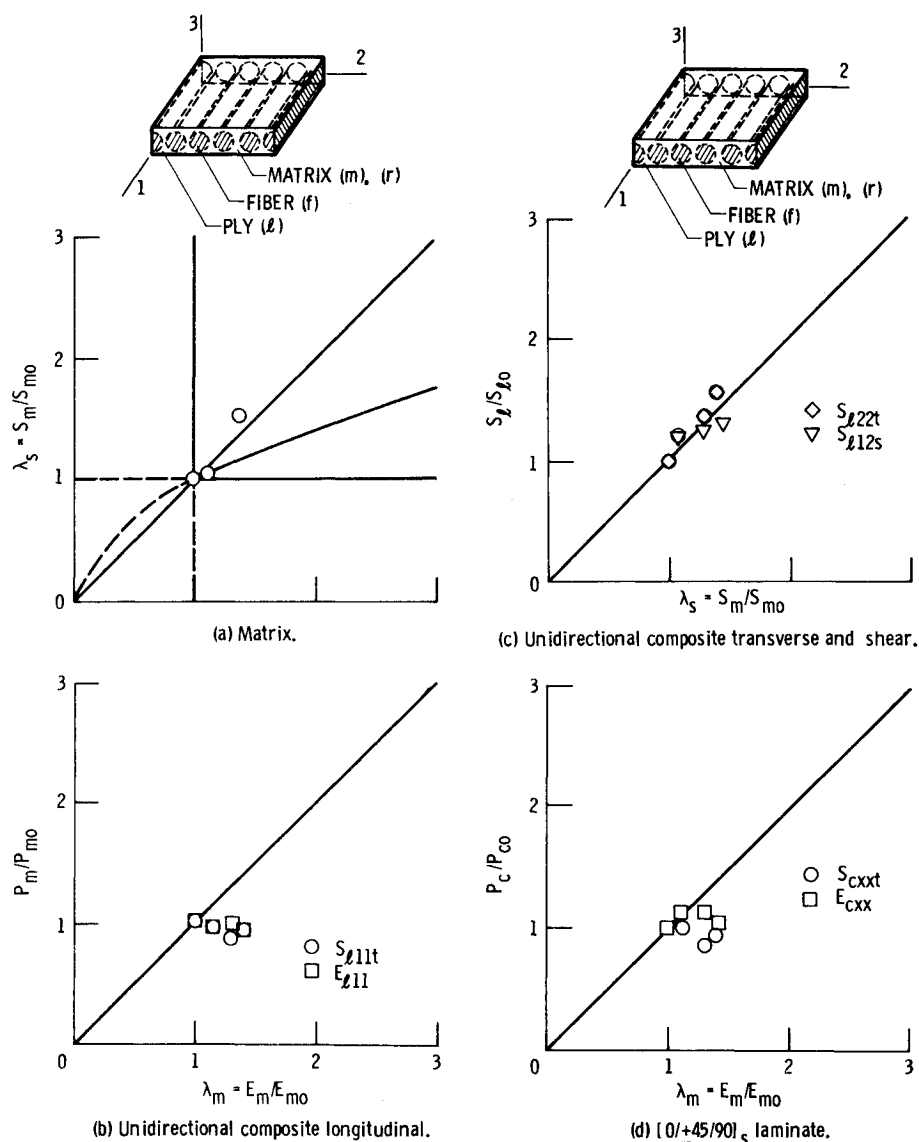


Fig. 16 Resin selection criteria correlation with measured composite data at elevated temperature.

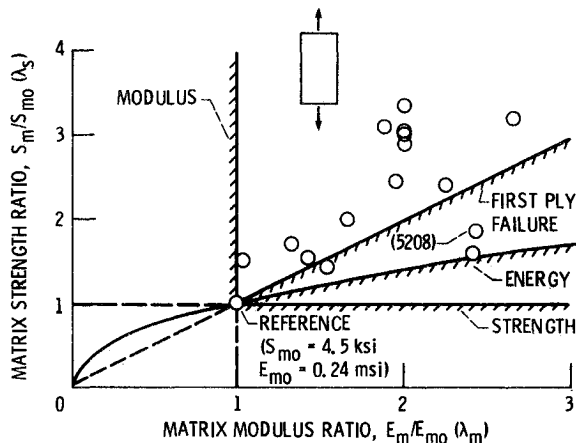


Fig. 17 Measured resin properties on selection criteria space.

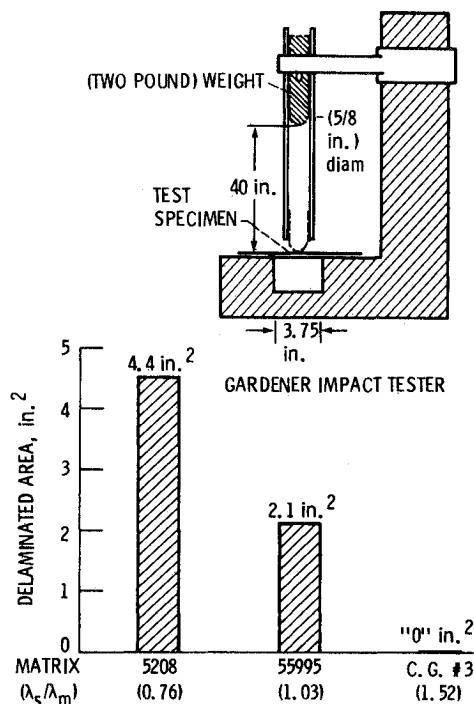


Fig. 18 Resin selection criteria correlation with impact-induced delaminated area $[(0/\pm 45/90) T300/resin]_s$.

Conclusions

Resin selection criteria for tougher composites were derived using a formal methodology consisting of upward integrated and top-down structured theories. The criteria account for resin strength and modulus, ply energy density, laminate first ply failure, and environmental and cyclic load effects. The criteria are expressed in resin properties benefits regions where the region boundaries are given by simplified equations, or ratios, for resin strength and modulus. The resin selection criteria correlate with experimental data for a

variety of conditions including laminate strength and stiffness, elevated temperature effects, and resistance to impact. The criteria, expressed in a criteria selection space, provide a formalized direction for the a priori selection and the development of resins for tougher composites.

References

- Chamis, C. C., Hanson, M. P., and Serafini, T. T., "Criteria for Selecting Resin Matrices for Improved Composite Strength," *Modern Plastics*, Vol. 50, May 1973, p. 90.
- Chamis, C. C., Lark, R. F., and Sinclair, J. H., "Integrated Theory for Predicting the Hygrothermomechanical Response of Advanced Composite Structural Components," *Advanced Composite Materials—Environmental Effects*, edited by J. R. Vinson, ASTM STP-658, Philadelphia, Pa., 1978, pp. 160-192.
- Chamis, C. C. and Sinclair, J. H., "Durability/Life of Fiber Composites in Hygrothermomechanical Environments," NASA TM-82749, 1981.
- Chamis, C. C., "Simplified Composite Micromechanics Equations for Hygral, Thermal and Mechanical Properties: *Proceedings of the SAMPE Quarterly*, Vol. 15, April 1984, pp. 14-23.
- Chamis, C. C., "Computerized Multilevel Analysis for Multilayered Fiber Composites," *Computers and Structures*, Vol. 3, May 1973, pp. 467-482.
- Chamis, C. D., "Vibration Characteristics of Composite Fan Blades and Comparison with Measured Data," *Journal of Aircraft*, Vol. 14, July 1977, pp. 644-647.
- Chamis, C. C. and Sinclair, J. H., "Analysis of High Velocity Impact on Hybrid Composite Fan Blades," *Journal of Aircraft*, Vol. 17, Oct. 1980, pp. 763-766.
- Chamis, C. C., "Buckling of Anisotropic Composite Plates," *Journal of the Structural Division, ASCE*, Vol. 95, Oct. 1969, pp. 2119-2139.
- Ashton, J. E. and Whitney, J. M., *Theory of Laminated Plates*, Technomic Publishing Co., Westport, Conn., 1970.
- Porter, T. R., "Environmental Effects on Defect Growth in Composite Materials, NASA CR-165213, 1981.
- Lekhnitskii, S. G., *Anizotropnye Plastinki (Anisotropic Plates)*, trans. from 2nd Russian ed. by S. W. Tsai and T. Cheron, Gordon and Breach Science Publishers, New York, 1968, p. 457.
- Daniel, I. M. and Liber, T., "Wave Propagation in Fiber Composite Laminates," IIT Research Institute, Chicago, Ill., IITRI-D6073-3-PT-2, NASA CR-135086, June 1976.
- Kim, B. S. and Moon, F. C., "Impact on Multilayered Composite Plates," NASA CR-135274, 1977.
- Yang, S. H. and Sun, C. T., "Indentation Law for Composite Laminates," Purdue University, Lafayette, Ind., CML-81-1, NASA CR-165460, July 1981.
- Chamis, C. C., "Failure Criteria for Filamentary Composites," *Composite Materials-Testing and Design*, ASTM STP-460, Philadelphia, Pa., 1969, pp. 336-351.
- Unpublished results, Lewis Research Center, 1981.
- Chamis, C. C., "Prediction of Fiber Composite Mechanical Behavior Made Simple," *Rising to the Challenge of the 80's*, Society of the Plastics Industry, Inc., New York, 1980, pp. 12-A-1-10.
- Chamis, C. C., "Sensitivity Analysis Results of the Effects of Various Parameters on Composite Design," *SAMPE Quarterly*, Vol. 14, Jan. 1983, pp. 1-6.
- Browning, C. E., Husman, G. E., and Whitney, J. M., "Moisture Effects in Epoxy Composites," *Composite Materials-Testing and Design*, ASTM STP-617, Philadelphia, Pa., 1977, pp. 481-496.
- Palmer, R. J., "Investigation of the Effect of Resin Materials on Impact Damage to Graphite/Epoxy Composites," NASA CR-165677, 1981.